



HAL
open science

Use of hydrogen bonded layer-by-layer assemblies for particle manipulation

C.C. Buron, T. Vrlicic, S. Lakard, F.E. Jurin, M. Quinart, S. Monney, B. Lakard

► **To cite this version:**

C.C. Buron, T. Vrlicic, S. Lakard, F.E. Jurin, M. Quinart, et al.. Use of hydrogen bonded layer-by-layer assemblies for particle manipulation. *Colloids and Surfaces A: Physicochemical and Engineering Aspects*, 2022, 648, pp.129251. 10.1016/j.colsurfa.2022.129251 . hal-03681242

HAL Id: hal-03681242

<https://hal.science/hal-03681242>

Submitted on 22 Jul 2024

HAL is a multi-disciplinary open access archive for the deposit and dissemination of scientific research documents, whether they are published or not. The documents may come from teaching and research institutions in France or abroad, or from public or private research centers.

L'archive ouverte pluridisciplinaire **HAL**, est destinée au dépôt et à la diffusion de documents scientifiques de niveau recherche, publiés ou non, émanant des établissements d'enseignement et de recherche français ou étrangers, des laboratoires publics ou privés.



Distributed under a Creative Commons Attribution - NonCommercial 4.0 International License

Use of hydrogen bonded layer-by-layer assemblies for particle manipulation

C.C. Buron*, T. Vrlinic, S. Lakard, F.E. Jurin, M. Quinart, S. Monney, B. Lakard

Univ. Bourgogne Franche-Comté, Institut UTINAM-UMR, CNRS 6213,
16 Route de Gray, 25030 Besançon cedex, France

*Corresponding author. Tel.: +33 3 81 66 59 25; E-mail address: cedric.buron@univ-fcomte.fr

ABSTRACT

With the constant progress in miniaturization of systems and devices, the manipulation of μ -objects is becoming increasingly important. Chemical functionalization is a promising way to improve this manipulation, in particular multilayer polymer films based on hydrogen bonds can allow to achieve reversible adhesion of μ -objects. To prepare such hydrogen-bonded Layer-by-Layer (LbL) films, poly(ethylene glycol) (PEG), poly(acrylic acid) (PAA), Tannic acid (TA) and Poly(N-isopropylacrylamide) carboxylic acid-terminated (PNIPAM) were selected due to their hydrogen donor or acceptor properties. . The growth of these films was originally confirmed by *in situ* optical reflectometry. Their erasability was also investigated by exposure to an aqueous solution with a pH gradient. Depending on the polymer couple, the pH of disintegration was adjusted from an acidic to a basic medium. The surface roughness was also affected by the building block of the LbL architecture since a rougher surface was recorded for PEG/TA than for PEG/PAA. To mimic the manipulation of an object, adsorption and desorption of a model object (silica particles) was carried out onto a LbL film. Two approaches were employed: optical reflectometry as an indirect method and optical microscopy for direct visualization. For both analyses, particles of different sizes could be adsorbed onto a PEG/PAA or PAA/PNIPAM film. Finally, a complete desorption of the particles was recorded due to the disintegration of the LbL film when the pH was increased.

Keywords: polymer multilayer films, hydrogen bonds, micromanipulation, optical reflectometry

INTRODUCTION

Thanks to the intense efforts made since the early 1990s, robotic manipulation is now mature at the macrometric scale. But a crucial challenge is now to be able to grasp and manipulate micro-objects in an accurate, reliable and repeatable manner as precision manipulation tasks are needed to replace manual operation with automated robotic micromanipulation in the biomedical and industrial fields. For this purpose, recent scientific advances of microtechnologies are crucial as they allow for the microfabrication of precision tools for the manipulation of micro-objects that can be useful for many potential applications including microassembly in robotics^{1, 2}, manipulation and characterization of bacteria³, embryos⁴ or neuronal cells⁵, drug delivery using biohybrid microrobots⁶, single-molecule micromanipulation for biophysical applications⁷, and microassembly of microstructures for the fabrication of MEMS.^{8, 9} Such micromanipulation tasks can be performed either with motor-driven grippers and end-effectors (contact micromanipulation) or with untethered physical fields (field micromanipulation). On the one hand, micro-grippers have finger openings allowing to handle μ -objects and achieve pick and place tasks, but releasing the object is still difficult and it is frequently necessary to introduce a liquid bridge between the gripper and the object to achieve this task^{10, 11}. AFM probes are also often used as end-effectors in force-controlled micromanipulation since the force that the probes apply to the object being manipulated can be accurately sensed and controlled^{12, 13}. On the other hand, in non-contact micromanipulation, the mechanical gripper is replaced by components generating a magnetic¹⁴⁻¹⁶, optical¹⁷⁻¹⁹, acoustic²⁰⁻²² or electric field²³⁻²⁵. While interesting achievements have been done with these techniques, such as the control of magnetically actuated micro-robots inside the eye for surgery and drug delivery¹⁴, these methods still suffer from a low blocking force (corresponding to the maximal force applied to an object without displacement), which is a major limitation since micromanipulation must be able to induce a significant force.

In order to develop more efficient micromanipulation tools than the existing ones, it is therefore necessary to put forward new strategies. Thus, the use of chemically modified grippers seems to be an interesting approach because of the use of functional chemical films deposited onto the gripper could allow to control the forces between the gripper and the object and thus to improve micromanipulation operations. In particular, pick-and-place micromanipulation of micro-objects could be greatly enhanced by the use of materials that change their properties in response to the application of various external stimuli (temperature, electric or magnetic stimuli, pH, chemical concentration, humidity, or light). For example, pick-and-place experiments have been achieved with a microgripper modified with a thermoresponsive hydrogel (N-isopropylacrylamide-co-acrylic acid) doped with magnetic nanoparticles.²⁶⁻²⁸ Another gripper used light absorption by black ink mixed

with polystyrene as a light stimulus leading to localized heating and inducing shrinkage of the structure and release of the object.²⁹ But until now, electroactive polymers, which are polymers reversibly deforming in response to electric stimuli, have been the most commonly used responsive materials for micromanipulation experiments.³⁰ Electroactive polymers consist of an electrolyte-swollen polymer membrane (a few hundred μm thick) sandwiched between two metallic electrodes. When a bias voltage (1-5 V) is applied to the electrodes, anions (cations) migrate to the anode (cathode), leading to a bending deformation of the system.^{31, 32} Using this methodology, a spherical metallic object with a mass of 15 mg was lifted up by microgrippers previously functionalized with an electroactive polymer.^{33, 34} The main advantage of this strategy is the ability to work in aqueous environments for applications such as sea exploration³⁵, drug delivery and surgical manipulation in body fluids.³⁶ However, these polymers still suffer from a slow response speed and low stress produced.³⁷

pH-sensitive polymers are a group of stimuli-responsive polymers that can respond to changes in solution pH by undergoing structural and property changes such as chain conformation, surface charge or solubility due to the presence of ionizable acidic or basic residues in their backbone. This class of materials has recently gained interest as they can be useful for many applications including gene^{38, 39} and drug delivery⁴⁰, (bio)sensors^{41, 42}, or filtration membranes.⁴³ Polyelectrolytes are typically described as pH-sensitive polymers as ionization of the monomers can be easily achieved by changing the solution pH (or ionic strength). Such a response to pH changes generally results in modifications of the physico-chemical properties of the polyelectrolytes which can be exploited to prepare grippers or actuators. Thus, pH-sensitive hydrogels based on polyelectrolytes have already been used to prepare soft actuators. For example, poly(acrylic acid) has been combined with hectorite clay to form a pH-responsive material allowing fast response and precise control of the acting direction, such as bidirectional bending flytrap, gel hand with grasp, and gesturing actions.⁴⁴ Similarly, poly(diallyldimethylammonium chloride) (PDDA) and poly(N-isopropylacrylamide) (PNIPAM) have been combined to prepare grippers for controlled delivery of small molecules and bilayer actuators showing unique bidirectional bending behaviour in response to pH changes.⁴⁵ Bio-bilayer hydrogels were also prepared from a solution of chitosan and cellulose/carboxymethylcellulose and demonstrated fast, reversible, and repeated self-rolling deformation actuated by pH-triggered swelling/deswelling. The significant difference in swelling behaviour between the positively charged chitosan and the negatively charged cellulose/carboxymethylcellulose layers generated sufficient force to actuate the performance of the hydrogels as soft grippers.⁴⁶ Another strategy for modifying interfaces with pH-sensitive polyelectrolytes consists in the assembly of multilayer films by the layer-by-layer method, developed by Decher⁴⁷, in which two species are alternately adsorbed onto a surface, resulting in the formation

of a nanometric thin film. Such assemblies have been extensively studied in the last 2 decades but only our group has used such polymer multilayer films to perform micromanipulation experiments. Indeed, we have recently succeeded in achieving reversible adhesion of borosilicate μ -spheres by grippers previously modified by a poly(acrylic acid) / polyethylene glycol (PAA/PEG) film based on hydrogen bonds.⁴⁸ More precisely, the μ -object was first grasped by the polymer multilayer-modified gripper in an aqueous environment (pH 2), then the pH of the solution was increased by the addition of NaOH, which causes the disassembly of the LbL film and the release of the μ -object at pH>4. In the work presented here, we propose to use two other pairs of polymers (PNIPAM/PAA and TA/PEG) to build LbL films based on hydrogen bonds and pH-responsive, and compare their behaviour with that of PEG/PAA films. Due to their different chemical structures, these polymer films can disassemble at different pH, thus offering the possibility to choose the disassembly pH depending on the targeted application. In this paper, the build-up of these polymer multilayer films and their evolution during pH changes is studied by optical reflectometry, while their structures are characterized by Atomic Force Microscopy. Finally, the adsorption/desorption of micrometric borosilicate spheres on a substrate is studied as a function of pH.

EXPERIMENTAL

Materials. Poly(acrylic acid) (PAA) having a M_w of 60 000 g/mol was purchased from Fluka Chemical Corp. Poly(ethylene glycol) (PEG), M_n of 35 000 g/mol, and Poly(N-isopropylacrylamide) carboxylic acid terminated (PNIPAM), M_n of 10 000 g/mol, were obtained from Sigma Aldrich. Tannic acid (TA) having a M_w of 1 701 g/mol was provided from Fischer Sci. Colloidal silica nanoparticles were purchased from AkzoNobel (BINDZIL, 30/220, 30 %, $d \approx 12$ nm) or synthesized in our laboratory ($r = 165$ nm) by the method described in detail previously.⁴⁹ Borosilicate glass spheres (BSG) ($r = 5 \mu\text{m}$) were provided from SPI Supplies. The polymer solutions were prepared in ultrapure water at 0.1 g/L and NaCl was added as a background electrolyte to set the ionic strength at 10^{-2} M. The nano and microparticle suspensions ($c = 0.01$ g/L) were also prepared in 10^{-2} M NaCl. For PAA/PEG, PEG/TA, and PAA/PNIPAM assemblies, the pH of the solution was set at 2. For both, pH was adjusted by addition of 1M HCl.

Polymer multilayer deposition. A conventional wafer cleaning procedure was employed to increase the density of SiOH groups on the silicon surface. The substrates were dipped in piranha solution (H_2SO_4 : $\text{H}_2\text{O}_2 = 3:1$, v/v) for 20 min and then extensively rinsed with ultrapure water. After cleaning, the substrates were vertically dipped into each polymer solution for 10 min. Three different types of assemblies were made: PEG/PAA, PAA/PNIPAM and PEG/TA. After assembly, the polymer films were dried in the open air for one day.

Optical reflectometry (OR). *In-situ* investigations of multilayer film assembly/disassembly were carried out by a home-made fixed-angle optical reflectometer. Adsorption was monitored through a change of polarization laser light. The beam was focused at a stagnation point of an impinging jet cell which was mounted directly on the reflectometer. The polymer solution was alternately injected using a constant flow rate. A signal, denoted S_0 , was first recorded during the injection of a free polymer solution and used as baseline. The raw data showed that the signal change, ΔS ie $S - S_0$, was directly linked to the amount of polymer adsorbed per unit area. No conversion of reflectometer output in adsorbed amount was done since the polymers have somewhat different refractive indices. Moreover, the composition of each layer in the multilayer films was unknown. Consequently, to compare experiments, the data were expressed as $\Delta S/S_0$.

During experiments, different information was obtained: i) the assembly profiles of various polymer couples, ii) the adsorption of nanoparticles onto the assembled films and iii) the depletion of the assembled films (+ particles) with pH. In the first step, the polymer solutions were alternately injected into the cell ($t = 10$ min) until the desired number of bilayers (N) was deposited. The assembly between PEG/PAA, PAA/PNIPAM and PEG/TA polymers was monitored. In the second step, a SiO_2 nanoparticles solution was injected into the cell directly after the polymer film assembly and their adsorption was followed during 10 min. Thus, films of $(\text{PEG/PAA})_N + \text{SiO}_2$ and $(\text{PAA/PNIPAM})_N + \text{SiO}_2$ were obtained. In the third step, the multilayer films with/without adsorbed particles were rinsed with 0.01 M NaCl solutions, whose pH was finally increased from pH 2 to pH 10 depending on the polymer couple.

Atomic Force Microscopy (AFM). A Nano-Observer atomic force microscope (CSI Instruments) was used to image the surface morphology after sample drying. Images were collected in contact mode using Pyrex-Nitride Probe Triangular Cantilevers, PNP-TR (spring constant 0.08 N/m, resonant frequency 17 kHz, Nano World). MountainsMap software from Digital Surf was used to treat pictures and determine roughness parameter. The root-mean-squared (rms) roughness was calculated by averaging 5 values collected from $400 \mu\text{m}^2$ areas on the AFM images.

Scanning Electron Microscopy (SEM). The scanning electron microscopy samples were observed with a high resolution FEG Digital Scanning Electron Microscope Leo982 Gemini from Zeiss. The samples were prepared by first depositing hydrogen-bonded films on silicon wafers ($N = 3$ bilayers). Afterwards, the wafers were rinsed in a 0.01 M NaCl solution at pH 2 and directly immersed into either nano or microparticle SiO_2 suspensions for 5 min. This step was followed by a second rinsing step (0.01 M NaCl at pH = 2) and drying under nitrogen flow. All samples were imaged after metallization.

Optical microscopy. Macroscopic surface observations were performed with a reflected light microscope having a 10× objective lens (Reichert Jung, Austria, model Polyvar-MET). Surface functionalization was done as previously described and the adsorption of borosilicate glass spheres was investigated as a function of the number of adsorbed bilayers. The views were finally recorded after exposure of the sample to a 0.01 M NaCl solution whose pH was set above the pH of hydrogen-bonded assembly destruction. This critical pH value for different assemblies was initially determined from optical reflectometry results.

RESULTS AND DISCUSSION

Growth and disintegration of polymer multilayers.

Optical reflectometry is a powerful tool to investigate the growth of a polymer film. Indeed, the assembly can be directly monitored during adsorption using a low polymer concentration. Consequently, this technique was initially employed to investigate the growth of hydrogen-bonded multilayers. Figure 1a shows the step-by-step adsorption of PEG and PAA at pH 2. Each step corresponds to the adsorption of one polymer. The solution containing PEG is the first one injected into the reflectometer cell. The reflectometry output increases followed by a plateau reflecting PEG adsorption. At pH 2, silicon oxide surface groups are predominantly non charged groups (silanol groups). So, hydrogen bonding can be established between the surface groups and the lone electron pair of oxygen of the ethyl oxide (EG) monomer. Then, when PAA is injected, reflectometry output increases again demonstrating the adsorption of PAA onto the PEG layer. The driving forces, as first demonstrated by Sukhishvili and Granick,⁵⁰ for PEG/PAA are as before hydrogen bonds which are created by the lone electron pair of oxygen of EG and the hydrogen of the carboxylic acid groups of PAA. Note that no conversion of $\Delta S/S_0$ was done and that the reflectometry output represents, at least semi-quantitatively, the amount of polymer adsorbed onto the SiO₂/Si substrate. A multilayer can also be constructed by starting with a PAA layer as shown in Figure 1b. Once again, a hydrogen bond is established between the silanol groups and the lone electron pair of oxygen available on the PAA monomer. By comparing the value of $\Delta S/S_0$ after the adsorption of 3 bilayers, the amount of adsorbed polymers seems to be higher for the PAA/PEG architecture than for the PEG/PAA one, that could be partially explained by a higher adsorption of PAA onto SiO₂. The growth mechanism of PEG/PAA seems to be exponential as demonstrated by the value recorded at the plateau for each polymer adsorption. This growth regime is due to the fact that PAA and PEG can form interpolymer complexes leading to an increase in the total adsorbed amount.⁵¹ The multilayer is then progressively exposed to a solution whose pH is progressively increased from 2 to 4 for 5 min. A strong decrease in

$\Delta S/S_0$ was noticed for the solution at pH 4 corresponding to the disassembly of the LbL films. This critical pH value is consistent with the value, e.g. pH 3.6, found for PAA/PEG disassembly in the literature.⁵² Indeed, the carboxylic acid groups begin to acquire a negative charge that disrupts hydrogen bonds and so the LbL architecture. More precisely, PEG has a nonionic nature, therefore its hydrogen bond acceptor properties are not affected by the pH of the assembly solution. At the opposite, PAA is a weak polyelectrolyte. Consequently, pH strongly influences the ratio of charged units and thus the assembly based on hydrogen bonds. As reported by Choi and Rubner⁵³, at pH 2, the carboxylic acid groups are fully protonated ($pK_a=6.5$) and the number of hydrogen bond donor sites is maximized. At pH 3.5, 5% of the carboxylic acid groups are charged and electrostatic repulsion is sufficient to initiate the destruction of hydrogen bonds.

For PAA/PNIPAM, reflectometry output clearly indicates the growth of a multilayer polymer film. After each injection of polymer solution at pH 2, an increase in $\Delta S/S_0$ can be noticed (Figure 2a). As for PEG/PAA, growth is also observed when the assembly starts with a PNIPAM layer (Figure 2b). In both cases, $(PAA/PNIPAM)_3$ or $(PNIPAM/PAA)_3$, the amount adsorbed is nearly the same.. Consequently, a hydrogen bond is established between silanol groups and PAA or PNIPAM. The construction of the film is ensured by the hydrogen bonding between the amide hydrogen of the PNIPAM and the carboxylic acid of the PAA.⁵⁴ Moreover the growth regime seems to be linear regarding the variation recorded at the end of each plateau. Exposure of films containing PAA and PNIPAM to a pH 7 solution leads to the disintegration of the film. So, the pH is much higher than for PAA/PEG. Indeed, as the pH increases, the deprotonation of the PAA monomers progressively increases but a hydrogen bond can still be established between the oxygen atom of PAA and the nitrogen atom of the amide hydrogen of PNIPAM. At pH 7, around 50-60 % of the carboxylic acid groups are ionized. Consequently, for PAA/PNIPAM, more repulsive interactions are needed to destroy the LbL architecture.

Finally, the assembly of PEG with TA is tested. As before, reflectometry experiments indicate that the assembly of PEG/TA works onto a silicon oxide substrate (Figure 3a and 3b). Surprisingly, for TA/PEG, no variation of $\Delta S/S_0$ is observed when TA is injected, thus indicating that no adsorption of TA onto the silanol groups is detected. So, Figure 3b represents the adsorption of 2.5 bilayers of TA/PEG rather than 3 bilayers. Moreover, for the same number of adsorbed layers, the amount adsorbed is the same. As for PEG/PAA, experiments show an exponential growth of the PEG/TA multilayer. The PEG/TA assembly was then rinsed with a pH 9 solution leading to the destruction of the films. This pH-triggered disintegration is similar to the work done by Erel-Unal and Sukhishvili where a PEG with a M_w of 200 000 g/mol was used.⁵⁵ TA is a polyphenol that can give rise to different types of interactions. Indeed, electrostatic, hydrogen bonding, and metal coordination have already been

reported.⁵⁶ At pH values below 8.5, TA is a hydrogen bond donor which can interact with the hydrogen bond acceptor of PEG. When the assembly is exposed to a solution at pH 9, above pK_a (8.5⁵⁵), the TA becomes a polyanion and electrostatic repulsion between the negative charges leads to a progressive disintegration of the multilayer as for the other couples.

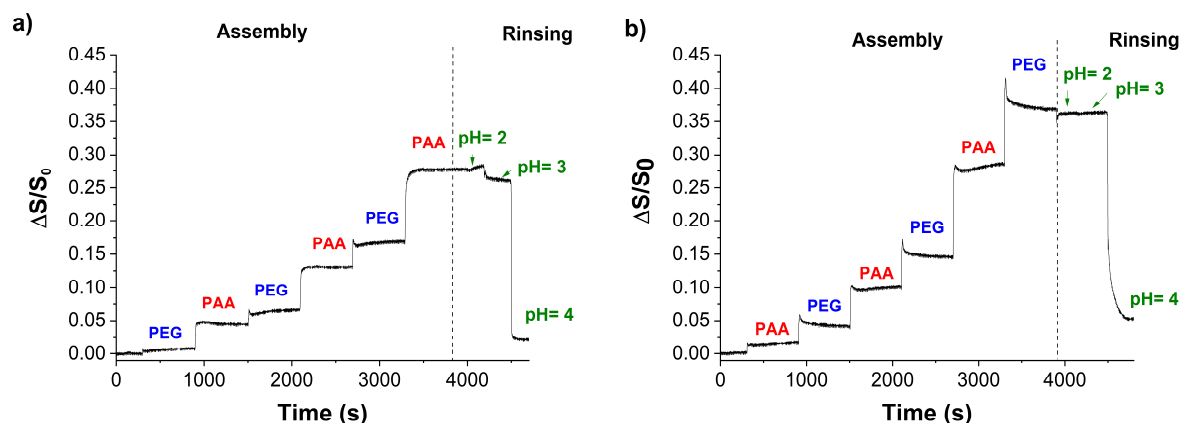


Figure 1: Growth/disintegration of (PEG/PAA)₃ and (PAA/PEG)₃ multilayers monitored by optical reflectometry ($C_{\text{polymer}} 0.1\text{g/L}$, NaCl 10^{-2}M , pH 2).

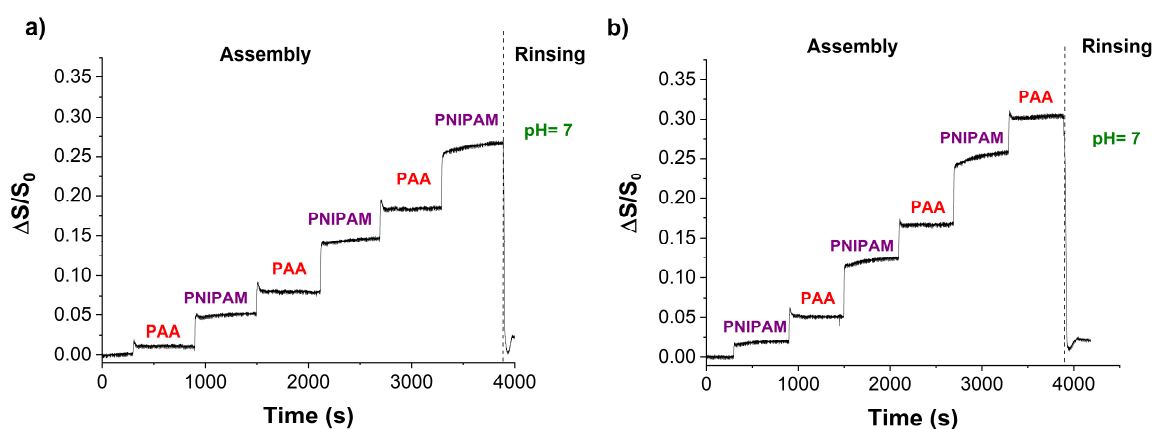


Figure 2 : Growth/disintegration of (PAA/PNIPAM)₃ and (PNIPAM/PAA)₃ multilayers monitored by optical reflectometry ($C_{\text{polymer}} 0.1\text{g/L}$, NaCl 10^{-2}M , pH 2).

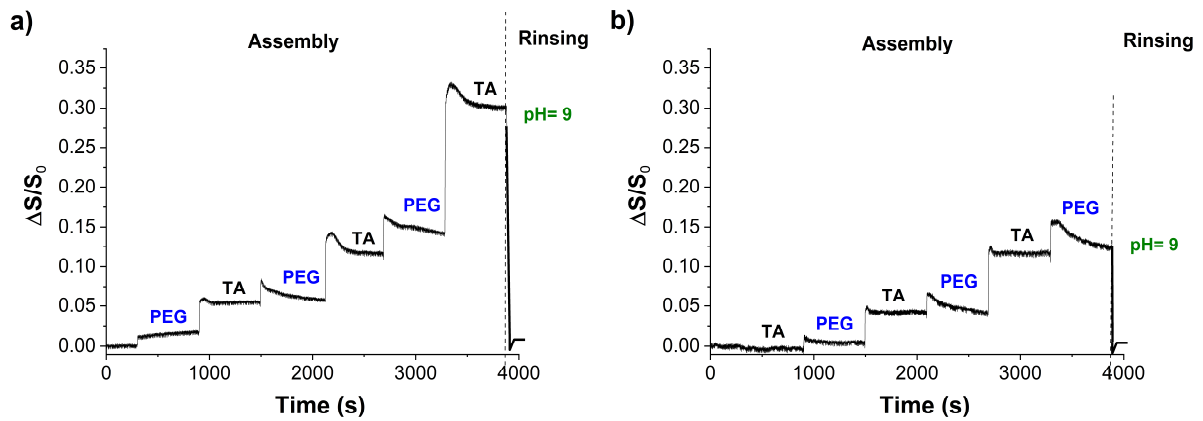


Figure 3 : Growth/disintegration of $(\text{PEG}/\text{TA})_3$ and $(\text{TA}/\text{PEG})_3$ multilayers monitored by optical reflectometry ($C_{\text{polymer}} 0.1\text{g/L}$, $\text{NaCl } 10^{-2}\text{M}$, $\text{pH } 2$).

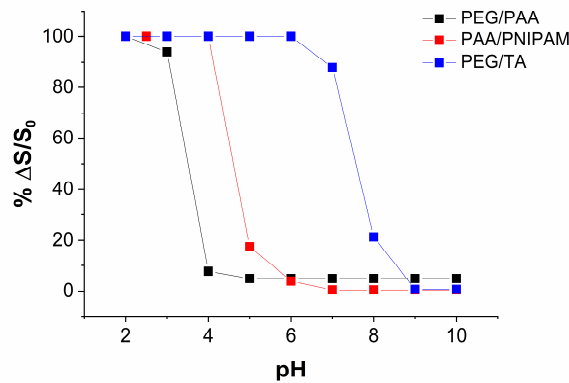


Figure 4 : Variation of reflectometry output during the rinsing step as a function of the pH and polymer couple. 100% corresponds to the reflectometry output after adsorption of 3 bilayers.

The erasability of the LbL film was investigated in detail as a function of the change in reflectometer output. After the multilayer growth, each architecture was exposed for 5 min to a solution with a pH increase from 2 to 10. Normalization of each desorption experiments was done from the $\Delta S/S_0$ value recorded after the deposition of 3 bilayers. The pH-triggered disintegration depends on the polymer couple used to prepare the film (Figure 4,). At pH 4, PEG/PAA is destroyed while a pH of 9 is required for PEG/TA. As explained previously in details, the dissociation of the hydrogen-bonded LbL film strongly depends on the balance between attractive and repulsive forces into the film when the pH of the solution is changed. So, the pK_a of the protonatable chemical function plays an important role. In the present case, the hydrogen-bonded multilayer appears to be an interesting way to functionalize a gripper to grasp and release μ -object in aqueous media. By choosing the polymer couple, the pH of disintegration can be selected from acidic to basic medium. In addition, if the μ -

object is degraded or corroded by the pH of the solution, another LbL functionalization can be used to perform its manipulation.

Multilayer film surface analysis.

After the growth analysis of the films and before to investigating the ability of each film to interact with a spherical μ -object, multilayer film surface morphology was studied using AFM. The 2D and 3D surface topographies of 3 bilayers obtained by assembly of PEG/PAA, PAA/PNIPAM and PEG/TA are presented in Figure 5. Note that the scale bars are the same for the different assemblies to facilitate the comparison (From 0 to 500 nm). A smooth surface with some globular islands is observed when PEG is combined with PAA. At the opposite, for films made of PEG and TA, a globular surface morphology was recorded. On average, the height of the globular shape is 2 to 5 times higher for PEG/TA than for PEG/PAA. The globules are also more distributed on the surface for the assembly made with TA. When PAA is combined with PNIPAM, the surface morphology is completely different. The film surface is relatively smooth but exhibits some very small islands 250 nm high. Consequently, the surface topography differs depending on the polymer couple and the globular structure is probably due to the use of PEG.

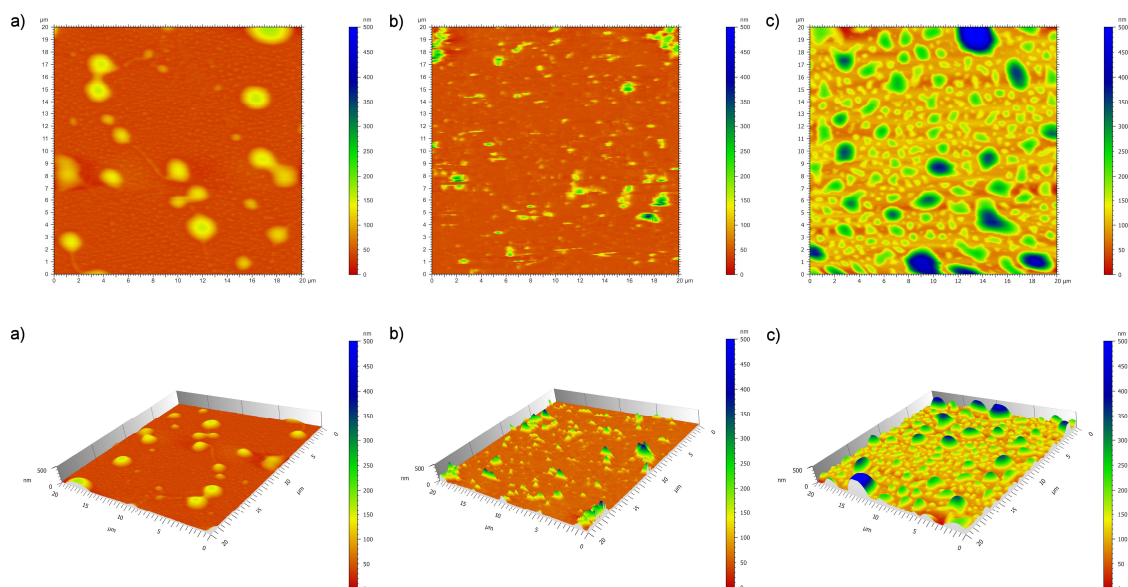


Figure 5 : AFM images showing 2D and 3D surface topographies of a) (PEG/PAA)₃, b) (PAA/PNIPAM)₃ and c) (PEG/TA)₃ hydrogen bonded assemblies.

Surface analysis was also carried out after the deposition of 1, 2, 5 and 8 bilayers. The average surface roughness, Sq, was then calculated and plotted in Figure 6 for each polymer couple. A quasi-

linear increase of roughness is observed whatever the assembly. However, a rough surface is produced when PEG is combined with TA. In detail, after adsorption of 8 bilayers, the surface roughness is equal to 93 nm for PEG/TA while it is equal to 21 nm for PEG/PAA. The variation in surface roughness variation is probably due to the difference between the molecular weight of each polymer and thus the number of monomers in each polymer chain. For PEG/PAA, the number of monomers is almost the same (795 for PEG and 600 for PAA) while for PNIPAM, the chain is made of 88 monomers. Finally, TA is a very small molecule having a molecular weight of 1701 g.mol⁻¹. Increasing the unbalance between polymer size leads to a rougher surface. Considering that a rough surface could be damaging for micromanipulation applications, the functionalization based on PEG/TA multilayer was abandoned. Indeed, the surface roughness reduces the number of interactions between the functionalized surface of the gripper and the μ -object and so to successfully grasp the object. As demonstrated by Tam *et al.* the surface roughness has the effect of reducing the area of contact between the surfaces and consequently reducing the interaction.⁵⁷

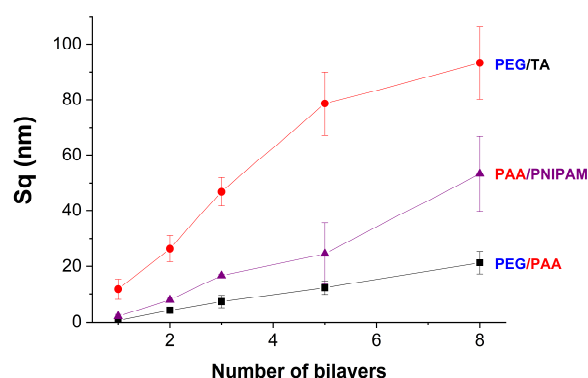


Figure 6 : Surface roughness of PEG/PAA, PAA/PNIPAM and PEG/TA hydrogen bonded assemblies.

Adsorption and desorption of particles

Knowing that the goal of this study is to grasp, move and release a μ -object, adsorption and desorption experiments of silica particles on top of a polymer film were done. Remember that the gripper will be functionalized by a hydrogen-bonded multilayer and the silica particle is a model object. Once again, optical reflectometry experiments were carried out first. To avoid a strong change in the reflectometry output due to the size of silica particles, colloidal silica nanoparticles with a diameter of 12 nm were employed. Before the injection of the solution containing nanoparticles, 3 bilayers of PEG/PAA were deposited on a silicon oxide substrate. As before (Figure 1), the output signal reaches a value around 0.26 showing a good repeatability of the LbL process

(Figure 7). Then, when the valve is turned to inject the particle solution, the output increases linearly. Silica particles which are not charged at pH 2 (closed to the point of zero charge, PZC) adsorb by hydrogen bonding. The surface of the particles is covered by silanol groups which can interact with the hydrogen of the PAA carboxyl groups. The plateau of adsorption, symbolizing the equilibrium, is not reached at the time scale of the experiment. Indeed, the adsorption kinetics of particle is very low in comparison with that of the polymer adsorption. Functionalization of the surface by the polymer and the size of the particles are known to alter the deposition of particles.^{58, 59} After 10 min, the substrate is rinsed with water solution at pH 2, 3, 4 and 5. The decrease in reflectometry output clearly indicates desorption of the silica particles due to the destruction of the LbL architecture. The pH leading to desorption seems to be higher when the particles are adsorbed. Indeed, in the first part, a pH of 4 is sufficient to erase the film while a pH of 5 is required to achieve desorption of the particles. To explore the possibility to functionalize the gripper again, a solution of PEG and PAA polymer at pH 2 is injected alternately without a drying step. The results in Figure 7 show that the LbL multilayer can redeposit onto the gripper which can grasp and release silica particles once again. The second part of the figure appears as a transposition of the first part.

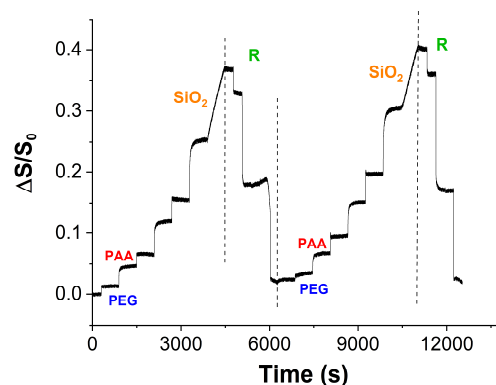


Figure 7 : Adsorption and desorption of silica nanoparticles on an erasable PEG/PAA multilayer (R: rinsing step, adsorption time: 10 min).

The same experiments were then carried out using PAA/PNIPAM multilayers (Figure 8). The adsorbed amount of PAA/PNIPAM and PNIPAM/PAA was almost the same (Figure 2), so it was arbitrary chosen to start the experiments with PAA injection. Only 2 bilayers were deposited before the adsorption of particles. Indeed, when 3 bilayers are adsorbed, oscillations of the output are recorded when particles are injected that prevent data processing. As for PEG/PAA, the adsorption of particle does not reach a plateau after 10 min and the variation of the output is linear. Desorption of the LbL structure is also visible when a pH 7 water solution is injected. As before, the critical pH for dissolution of the LbL film seems to be higher when particles are adsorbed onto the film. The second

part of Figure 8 indicates that an additional functionalization can be done with the same erasable properties.

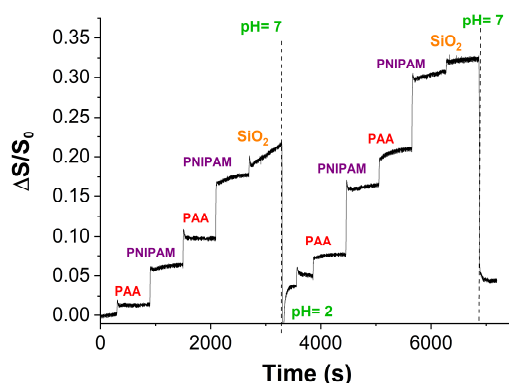


Figure 8 : Adsorption and desorption of silica nanoparticles on an erasable PAA/PNIPAM multilayer.

Particle adsorption: Effect of the particle size

Reflectometry is an indirect technique to monitor the adsorption of different materials. To observe how the particles are adsorbed, SEM images were carried out. PEG/PAA and PAA/PNIPAM couples were both tested. The possibility to grasp a spherical object of different sizes was also investigated using two sizes of silica particles: one in the nanometer range, *i.e.* 300 nm, and another one in the micrometer scale, *i.e.* 10 μm . The images presented in Figure 9 confirm that whatever the hydrogen-bonded polymer film, adsorption of particle is observed. The particle size does seem to be a critical parameter. Indeed, 300 nm and 10 μm silica particles are visible in the SEM images. The surface coverage of the particles is higher for the PEG/PAA multilayer (Figure 9a,b) than for the PAA/PNIPAM multilayer (Figure 9c,d). The density of -OH groups on the surface of the polymer film is probably lower for the PAA/PNIPAM based architecture. This is in a good agreement with reflectometry experiments where the adsorbed amount of silica particles is higher when deposited onto a PEG/PAA multilayer. As shown by Lutkenhaus *et al.*, at lower pH, PAA tends to bind to itself, reducing its ability to bind to PEG. An increase in the PAA content into the film is thus recorded.⁶⁰ Consequently, PEG/PAA functionalization should be preferred to maximize the probability to grasp an object. More generally, the reflectometry experiments are so corroborated by the SEM observations. The strategy consisting in the formation of hydrogen bonds between a polymer film and a spherical object seems to be independent of the size of the spherical object.

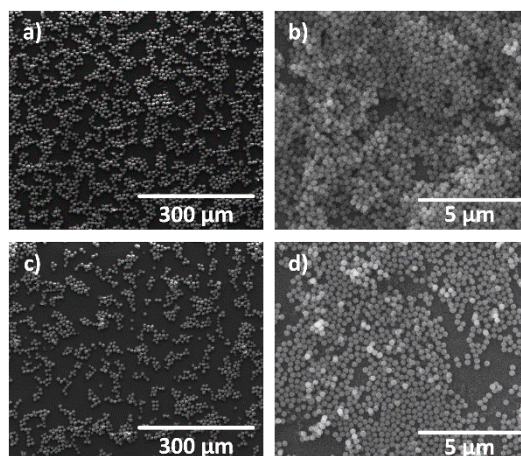


Figure 9 : SEM observations of a) SiO₂ 10 μm b) SiO₂ 300 nm adsorbed on the top of (PEG/PAA)₃ and c) SiO₂ 10 μm d) SiO₂ 300 nm adsorbed on the top of (PAA/PNIPAM)₃.

Mimicking of micro-object capture and release.

Adsorption/desorption of silica particles (10 μm) onto PEG/PAA and PAA/PNIPAM multilayers composed of N bilayers was finally observed by optical microscopy. The number of deposited layers is always an even number meaning that the particles are adsorbed on the PAA polymer or PNIPAM polymer. As depicted in Figure 10 and Figure 11, the number of adsorbed particles clearly depends on the number of bilayers N. For N=1, the particles are spread onto the substrate surface and form some aggregates. Only a few particles are observed individually. At the opposite, for N=8, the substrate is covered by a homogeneous coating. Note that the images were done in liquid media without drying to mimic the micromanipulation process. Similar to SEM investigations, the surface coverage of particles is lower for PAA/PNIPAM functionalization. Then, each sample was immersed into a pH 10 solution for 10 min.

For PEG/PAA, immersion into a basic solution leads to a complete removal of silica particles from the substrate for N = 3, 5 and 8 due to the destruction of hydrogen-bonded multilayer. For N = 1 and 2, it seems that some particles are still stuck onto the substrate even after immersion in a basic medium. Considering that for a few adsorbed polymer layers, the PEG/PAA LbL film does not cover the entire silicon substrate, the particles are probably adsorbed onto the silicon substrate by hydrogen bonding. As the pH increases, the surface charge of both the adsorbed particles and the silicon oxide thin layer on top of the silicon wafer increases. Consequently, repulsive interactions should lead to complete desorption of the particles, unless strong interactions were initially created during the adsorption step. Indeed, between a spherical particle and a planar substrate, van der Waals interactions could arise, in addition to hydrogen bonding if the distance is small enough. However, van der Waals forces

do not depend on the surface charge and are therefore insensitive to pH modification, that could explain the presence of some remaining particles onto the substrate. For PAA/PNIPAM, immersion into a basic solution leads to a complete removal of silica particles from the substrate for N = 1, 2, 3 and 5. For 8 bilayers, some particles are still attached to the substrate and the surface appears to be inhomogeneous. Considering that there is no convection in these experiments, the PAA/PNIPAM LbL film is not completely destroyed. The pH of 10 is probably too weak to lead to a complete desorption of the thick film knowing that the destruction begins at pH 7 for the PAA/PNIPAM couple.

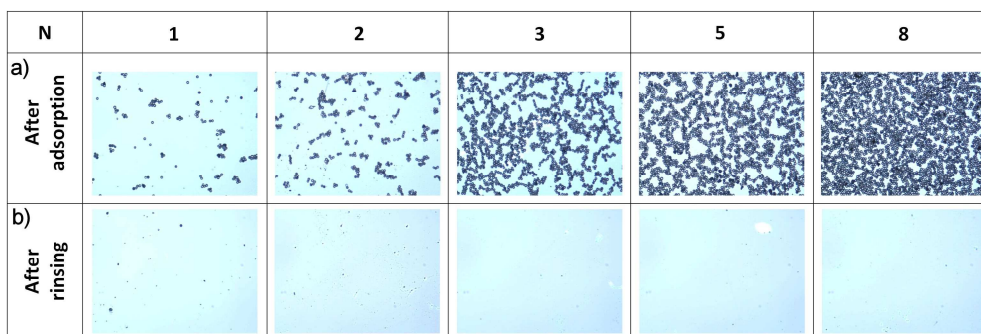


Figure 10: a) Images of silica particles (10 μm) adsorbed on PEG/PAA multilayer film made of N bilayers at pH 2 and NaCl 0.01M b) Images recorded after a rinsing step of the previous samples with a solution of NaCl 0.01M at pH 10. The images size is 700 μm \times 930 μm .

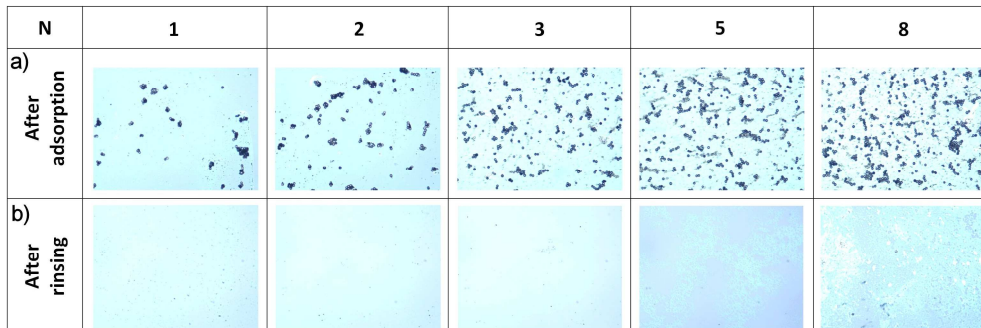


Figure 11: a) Images of silica particles (10 μm) adsorbed on PAA/PNIPAM multilayer film made of N bilayers at pH 2 and NaCl 0.01M b) Images recorded after a rinsing step of the previous samples with a solution of NaCl 0.01M at pH 10. The images size is 700 μm \times 930 μm .

CONCLUSION

In the present work, the deposition and disintegration of LbL films based on the assembly of 3 different polymer couples were investigated. These experiments were done to evidence the possibility of using the hydrogen-bonded multilayer functionalization to capture, displace and release a micro-object in aqueous solution.

Reflectometry experiments successfully demonstrated the capability of growing a multilayer onto a silicon oxide substrate. For PEG/PAA and PAA/PNIPAM couples, the growth was recorded whatever the first polymer injected into the cell. Conversely, TA doesn't appear to be adsorbed onto silanol surface groups. The pH of disintegration, due to the rupture of hydrogen bonds, strongly depends on the couple of polymers which allows to consider μ -manipulations operations at different pH. Moreover, the desorption of the film is fast and no convection is needed. To mimic the grasping of a micro-object by a gripper functionalized by a H-bonding film, nanoparticles of silica were injected into the reflectometer cell. Particle adsorption onto PEG/PAA and PAA/PNIPAM was clearly observed as well as their desorption when the pH of the rinsing solution was increased. It is also easy to reconstruct the LbL film directly after its disintegration without a rinsing step showing that the system could be reused several times. SEM images confirmed that particles can also be adsorbed whatever their size. Finally, direct observations of particle desorption and so LbL disintegration were done by optical microscopy. For PEG/PAA and PAA/PNIPAM, the desorption is nearly complete whatever the number of adsorbed bilayers. Hydrogen bonded LbL functionalization is so a promising route to modify gripper and displace objects in a liquid medium. In future studies, these easily prepared hydrogen-bonded films will be used to functionalize an AFM tip in order to grasp, move, and release object of different sizes and different chemical natures.

ACKNOWLEDGMENTS

This work was supported by a grant of the French National Agency (ANR), project number: ANR-13-JS08-0009-01.

REFERENCES

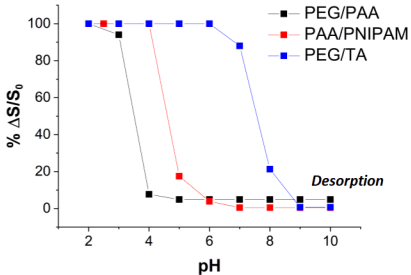
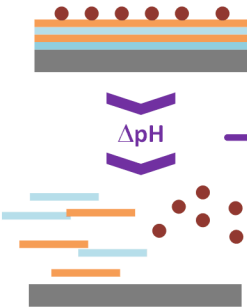
1. Hines, L.; Petersen, K.; Lum, G. Z.; Sitti, M., Soft Actuators for Small-Scale Robotics. *Advanced Materials* **2017**, *29* (13), 1603483.
2. Zhang, Z.; Wang, X.; Liu, J.; Dai, C.; Sun, Y., Robotic Micromanipulation: Fundamentals and Applications. *Annual Review of Control, Robotics, and Autonomous Systems* **2019**, *2* (1), 181-203.
3. Schröder, U.-C.; Glaser, U.; Leiterer, C.; Csaki, A.; Fritzsche, W.; Bauer, M.; Popp, J.; Neugebauer, U., Micromanipulation of sepsis relevant bacteria with dielectrophoresis. *Infection* **2011**, *39*, S104-S105.
4. Halvaei, I.; Ghazali, S.; Nottola, S. A.; Khalili, M. A., Cleavage-stage embryo micromanipulation in the clinical setting. *Systems Biology in Reproductive Medicine* **2018**, *64* (3), 157-168.
5. Stuhmann, B.; Gögler, M.; Betz, T.; Ehrlicher, A.; Koch, D.; Käs, J., Automated tracking and laser micromanipulation of motile cells. *Review of Scientific Instruments* **2005**, *76* (3), 035105.
6. Felfoul, O.; Mohammadi, M.; Taherkhani, S.; de Lanauze, D.; Zhong Xu, Y.; Loghin, D.; Essa, S.; Jancik, S.; Houle, D.; Lafleur, M.; Gaboury, L.; Tabrizian, M.; Kaou, N.; Atkin, M.; Vuong, T.; Batist, G.; Beauchemin, N.; Radzioch, D.; Martel, S., Magneto-aerotactic bacteria deliver drug-containing nanoliposomes to tumour hypoxic regions. *Nat Nanotechnol* **2016**, *11* (11), 941-947.

7. Neuman, K. C.; Lionnet, T.; Allemand, J.-F., Single-Molecule Micromanipulation Techniques. *Annual Review of Materials Research* **2007**, *37* (1), 33-67.
8. Dechev, N.; Cleghorn, W. L.; Mills, J. K., Microassembly of 3-D microstructures using a compliant, passive microgripper. *Journal of Microelectromechanical Systems* **2004**, *13* (2), 176-189.
9. Ghadiri, R.; Weigel, T.; Esen, C.; Ostendorf, A., Microassembly of complex and three-dimensional microstructures using holographic optical tweezers. *Journal of Micromechanics and Microengineering* **2012**, *22* (6), 065016.
10. Fan, Z.; Rong, W.; Wang, L.; Sun, L., A single-probe capillary microgripper induced by dropwise condensation and inertial release. *Journal of Micromechanics and Microengineering* **2015**, *25*, 115011.
11. Vasudev, A.; Jagtiani, A.; Du, L.; Zhe, J., A low-voltage droplet microgripper for micro-object manipulation. *Journal of Micromechanics and Microengineering* **2009**, *19* (7), 075005.
12. Xie, H.; Régnier, S., Development of a Flexible Robotic System for Multiscale Applications of Micro/Nanoscale Manipulation and Assembly. *IEEE/ASME Transactions on Mechatronics* **2011**, *16* (2), 266-276.
13. Xie, H.; Zhang, H.; Song, J.; Meng, X.; Wen, Y.; Sun, L., High-Precision Automated Micromanipulation and Adhesive Microbonding With Cantilevered Micropipette Probes in the Dynamic Probing Mode. *IEEE/ASME Transactions on Mechatronics* **2018**, *23*, 1425-1435.
14. de Ávila, B. E.-F.; Angsantikul, P.; Li, J.; Angel Lopez-Ramirez, M.; Ramírez-Herrera, D. E.; Thamphiwatana, S.; Chen, C.; Delezuk, J.; Samakapiruk, R.; Ramez, V.; Obonyo, M.; Zhang, L.; Wang, J., Micromotor-enabled active drug delivery for in vivo treatment of stomach infection. *Nature Communications* **2017**, *8* (1), 272.
15. Wang, X.; Luo, M.; Ho, C.; Zhang, Z.; Zhao, Q.; Dai, C.; Sun, Y., Robotic Intracellular Manipulation: 3D Navigation and Measurement Inside a Single Cell. *2018 IEEE International Conference on Robotics and Automation (ICRA)* **2018**, 2716-2721.
16. Zhang, L.; Abbott, J. J.; Dong, L.; Kratochvil, B. E.; Bell, D.; Nelson, B. J., Artificial bacterial flagella: Fabrication and magnetic control. *Applied Physics Letters* **2009**, *94* (6), 064107.
17. Chen, T.; Shi, L. Z.; Zhu, Q.; Chandsawangbhuwana, C.; Berns, M. W., Optical tweezers and non-ratiometric fluorescent-dye-based studies of respiration in sperm mitochondria. *Journal of Optics* **2011**, *13* (4), 044010.
18. Leach, J.; Howard, D.; Roberts, S.; Gibson, G.; Gothard, D.; Cooper, J.; Shakesheff, K.; Padgett, M.; Buttery, L., Manipulation of live mouse embryonic stem cells using holographic optical tweezers. *Journal of Modern Optics* **2009**, *56* (4), 448-452.
19. Li, X.; Liu, C.; Chen, S.; Wang, Y.; Cheng, S. H.; Sun, D., *In Vivo* Manipulation of Single Biological Cells With an Optical Tweezers-Based Manipulator and a Disturbance Compensation Controller. *IEEE Transactions on Robotics* **2017**, *33* (5), 1200-1212.
20. Guo, F.; Mao, Z.; Chen, Y.; Xie, Z.; Lata, J. P.; Li, P.; Ren, L.; Liu, J.; Yang, J.; Dao, M.; Suresh, S.; Huang, T. J., Three-dimensional manipulation of single cells using surface acoustic waves. *Proc Natl Acad Sci U S A* **2016**, *113* (6), 1522-7.
21. Li, P.; Mao, Z.; Peng, Z.; Zhou, L.; Chen, Y.; Huang, P. H.; Truica, C. I.; Drabick, J. J.; El-Deiry, W. S.; Dao, M.; Suresh, S.; Huang, T. J., Acoustic separation of circulating tumor cells. *Proc Natl Acad Sci U S A* **2015**, *112* (16), 4970-5.
22. Samandari, M.; Abrinia, K.; Sanati-Nezhad, A., Acoustic Manipulation of Bio-Particles at High Frequencies: An Analytical and Simulation Approach. *Micromachines (Basel)* **2017**, *8* (10), 290.
23. Kumemura, M.; Collard, D.; Sakaki, N.; Yamahata, C.; Hosogi, M.; Hashiguchi, G.; Fujita, H., Single-DNA-molecule trapping with silicon nanotweezers using pulsed dielectrophoresis. *Journal of Micromechanics and Microengineering* **2011**, *21* (5), 054020.
24. Lownes Urbano, R.; Morss Clyne, A., An inverted dielectrophoretic device for analysis of attached single cell mechanics. *Lab on a Chip* **2016**, *16* (3), 561-573.
25. Velev, O. D.; Bhatt, K. H., On-chip micromanipulation and assembly of colloidal particles by electric fields. *Soft Matter* **2006**, *2* (9), 738-750.

26. Ongaro, F.; Scheggi, S.; Yoon, C.; den Brink, F. v.; Oh, S. H.; Gracias, D. H.; Misra, S., Autonomous planning and control of soft untethered grippers in unstructured environments. *Journal of Micro-Bio Robotics* **2017**, *12* (1), 45-52.
27. Illés, E.; Szekeres, M.; Tóth, I. Y.; Szabó, Á.; Iván, B.; Turcu, R.; Vékás, L.; Zupkó, I.; Jaics, G.; Tombácz, E., Multifunctional PEG-carboxylate copolymer coated superparamagnetic iron oxide nanoparticles for biomedical application. *Journal of Magnetism and Magnetic Materials* **2018**, *451*, 710-720.
28. Illés, E.; Tombácz, E.; Szekeres, M.; Tóth, I. Y.; Szabó, Á.; Iván, B., Novel carboxylated PEG-coating on magnetite nanoparticles designed for biomedical applications. *Journal of Magnetism and Magnetic Materials* **2015**, *380*, 132-139.
29. Hubbard, A. M.; Mailen, R. W.; Zikry, M. A.; Dickey, M. D.; Genzer, J., Controllable curvature from planar polymer sheets in response to light. *Soft Matter* **2017**, *13* (12), 2299-2308.
30. Shahinpoor, M.; Kim, K. J., Ionic polymer-metal composites: I. Fundamentals. *Smart Materials and Structures* **2001**, *10* (4), 819-833.
31. Kim, S. J.; Pugal, D.; Wong, J.; Kim, K. J.; Yim, W., A bio-inspired multi degree of freedom actuator based on a novel cylindrical ionic polymer–metal composite material. *Robotics and Autonomous Systems* **2014**, *62* (1), 53-60.
32. Nemat-Nasser, S.; Wu, Y., Comparative experimental study of ionic polymer–metal composites with different backbone ionomers and in various cation forms. *Journal of Applied Physics* **2003**, *93* (9), 5255-5267.
33. Deole, U.; Lumia, R.; Shahinpoor, M.; Bermudez, M., Design and test of IPMC artificial muscle microgripper. *Journal of Micro-Nano Mechatronics* **2008**, *4* (3), 95-102.
34. Lumia, R.; Shahinpoor, M., IPMC microgripper research and development. *Journal of Physics: Conference Series* **2008**, *127*, 012002.
35. Galloway, K. C.; Becker, K. P.; Phillips, B.; Kirby, J.; Licht, S.; Tchernov, D.; Wood, R. J.; Gruber, D. F., Soft Robotic Grippers for Biological Sampling on Deep Reefs. *Soft Robotics* **2016**, *3* (1), 23-33.
36. Ghosh, A.; Yoon, C.; Ongaro, F.; Scheggi, S.; Selaru, F. M.; Misra, S.; Gracias, D. H., Stimuli-Responsive Soft Untethered Grippers for Drug Delivery and Robotic Surgery. *Front Mech Eng* **2017**, *3*, 7.
37. Shintake, J.; Cacucciolo, V.; Floreano, D.; Shea, H., Soft Robotic Grippers. *Advanced Materials* **2018**, *30* (29), 1707035.
38. Yuba, E., Design of pH-sensitive polymer-modified liposomes for antigen delivery and their application in cancer immunotherapy. *Polymer Journal* **2016**, *48* (7), 761-771.
39. Yuba, E.; Kono, Y.; Harada, A.; Yokoyama, S.; Arai, M.; Kubo, K.; Kono, K., The application of pH-sensitive polymer-lipids to antigen delivery for cancer immunotherapy. *Biomaterials* **2013**, *34* (22), 5711-5721.
40. Tang, H.; Guo, J.; Sun, Y.; Chang, B.; Ren, Q.; Yang, W., Facile synthesis of pH sensitive polymer-coated mesoporous silica nanoparticles and their application in drug delivery. *International Journal of Pharmaceutics* **2011**, *421* (2), 388-396.
41. Cai, Q.; Zeng, K.; Ruan, C.; Desai, T. A.; Grimes, C. A., A Wireless, Remote Query Glucose Biosensor Based on a pH-Sensitive Polymer. *Analytical Chemistry* **2004**, *76* (14), 4038-4043.
42. Niece, K. L., A pH-Sensitive Polymer Sensor Developed. *MRS Bulletin* **2006**, *31* (2), 79-80.
43. Lakard, S.; Magnenet, C.; Mokhter, M. A.; Euvrard, M.; Buron, C. C.; Lakard, B., Retention of Cu(II) and Ni(II) ions by filtration through polymer-modified membranes. *Separation and Purification Technology* **2015**, *149*, 1-8.
44. Zhao, L.; Huang, J.; Zhang, Y.; Wang, T.; Sun, W.; Tong, Z., Programmable and Bidirectional Bending of Soft Actuators Based on Janus Structure with Sticky Tough PAA-Clay Hydrogel. *ACS applied materials & interfaces* **2017**, *9* (13), 11866-11873.
45. Li, X.; Cai, X.; Gao, Y.; Serpe, M. J., Reversible bidirectional bending of hydrogel-based bilayer actuators. *Journal of Materials Chemistry B* **2017**, *5* (15), 2804-2812.

46. Duan, J.; Liang, X.; Zhu, K.; Guo, J.; Zhang, L., Bilayer hydrogel actuators with tight interfacial adhesion fully constructed from natural polysaccharides. *Soft Matter* **2017**, *13* (2), 345-354.
47. Decher, G., Fuzzy Nanoassemblies: Toward Layered Polymeric Multicomposites. *Science* **1997**, *277* (5330), 1232-1237.
48. Buron, C. C.; Vrlinic, T.; Le Gallou, T.; Lakard, S.; Bolopion, A.; Rougeot, P.; Lakard, B., pH-Responsive PEG/PAA Multilayer Assemblies for Reversible Adhesion of Micro-Objects. *ACS Applied Polymer Materials* **2020**, *2* (12), 5646-5653.
49. Roosz, N.; Euvard, M.; Lakard, B.; Buron, C. C.; Martin, N.; Viau, L., Synthesis and characterization of polyaniline-silica composites: Raspberry vs core-shell structures. Where do we stand? *Journal of Colloid and Interface Science* **2017**, *502*, 184-192.
50. Sukhishvili, S. A.; Granick, S., Layered, Erasable Polymer Multilayers Formed by Hydrogen-Bonded Sequential Self-Assembly. *Macromolecules* **2002**, *35* (1), 301-310.
51. Szabó, Á.; Szanka, I.; Tolnai, G.; Szarka, G.; Iván, B., LCST-type thermoresponsive behaviour of interpolymer complexes of well-defined poly(poly(ethylene glycol) methacrylate)s and poly(acrylic acid) synthesized by ATRP. *Polymer* **2017**, *111*, 61-66.
52. Sukhishvili, S. A.; Granick, S., Layered, Erasable, Ultrathin Polymer Films. *Journal of the American Chemical Society* **2000**, *122* (39), 9550-9551.
53. Choi, J.; Rubner, M. F., Influence of the degree of ionization on weak polyelectrolyte multilayer assembly. *Macromolecules* **2005**, *38* (1), 116-124.
54. Quinn, J. F.; Caruso, F., Facile Tailoring of Film Morphology and Release Properties Using Layer-by-Layer Assembly of Thermoresponsive Materials. *Langmuir* **2004**, *20* (1), 20-22.
55. Erel-Unal, I.; Sukhishvili, S. A., Hydrogen-Bonded Multilayers of a Neutral Polymer and a Polyphenol. *Macromolecules* **2008**, *41* (11), 3962-3970.
56. Ringwald, C.; Ball, V., Layer-by-layer deposition of tannic acid and Fe³⁺ cations is of electrostatic nature but almost ionic strength independent at pH 5. *Journal of Colloid and Interface Science* **2015**, *450*, 119-126.
57. Tam, E.; Sausse Lhernould, M.; Lambert, P.; Delchambre, A.; Delplancke-Ogletree, M.-P., Electrostatic forces in micromanipulation: Experimental characterization and simulation including roughness. *Applied Surface Science* **2009**, *255* (18), 7898-7904.
58. Böhmer, M. R., Effects of polymers on particle adsorption on macroscopic surfaces studied by optical reflectometry. *Journal of Colloid and Interface Science* **1998**, *197* (2), 251-256.
59. Elimelech, M., Kinetics of capture of colloidal particles in packed beds under attractive double layer interactions. *Journal of Colloid and Interface Science* **1991**, *146* (2), 337-352.
60. Lutkenhaus, J. L.; McEnnis, K.; Hammond, P. T., Tuning the Glass Transition of and Ion Transport within Hydrogen-Bonded Layer-by-Layer Assemblies. *Macromolecules* **2007**, *40* (23), 8367-8373.

Layer-by-Layer polymer assembly and disintegration



Particle release